Kuwait J. Sci. Eng. **33**(1) pp. 155-168, 2006

Shear stress distributions along the cross section in smooth and rough open channel flows

MEHMET ARDIÇLIOĞLU[1], GALİP SEKÇİN[2],
AND RECEP YURTAL[2]

[1]*Department of Civil Engineering, Faculty of Engineering, The Erciyes University, Kayseri, Turkey, E-mail: mardic@erciyes.edu.tr*

[2]*Department of Environmental and Civil Engineering, Faculty of Engineering, The Çukurova University, Adana, Turkey.*

ABSTRACT

Distributions of shear stresses throughout the entire cross-section within the fully developed boundary layer region in both the smooth and rough surfaces of a rectangular open channel flow were experimentally determined. Velocity measurements were taken for two different surfaces and 48 flow conditions with Froude numbers in the range: $0.12 \leq Fr \leq 1.23$ and with aspect ratios within: $4.2 \leq b/h \leq 21.6$. For all the flow conditions created in the setup, the local shear stress was computed using the universal logarithmic distribution. The relationships between the mean cross sectional shear stresses and the aspect ratio, and Froude numbers were determined for both smooth and rough surfaces. For all the flow conditions formed in the setup, the shear stress distribution along the cross section was succinctly expressed by a second degree polynomial. The maximum shear stress on the bed was found to be about 6-20% greater than the mean bed shear stress for smooth surfaces and 2-16% grater for rough surfaces, respectively.

Key words: open channel flow, shear stress distributions, smooth and rough surfaces.

INTRODUCTION

Determination of the boundary shear stress and its distribution along the wetted perimeter is one of the basic problems in open channel flow. Shear stress distribution is related to the computation of flow resistance, side wall correction, sediment transport rate, channel erosion or deposition, and design of channels.

The boundary shear stress distribution and flow resistance in both compound and singular cross-section channels with smooth and rough surfaces have been investigated by many scientists (Knight & Patel 1985, Nezu *et al.* 1993, Rhodes & Knight 1994, Biron *et al.* 1997, Zheng & Jin 1998, Ackerman & Hoover 2001). Abaza and Al-Khatip (2002) experimentally tested five different types of

boundary shear stress distributions in a symmetrical rectangular compound channel. A generalized multi-variety regression model has been derived to predict each experimentally measured shear stress as a function of three dimensionless parameters.

Knight *et al.* (1994) presented equations to quantify the mean and maximum boundary shear stresses separately for those acting on the bed, τ_b, and on the walls, τ_w, for straight trapezoidal channels. They made no attempt to specify the lateral distributions of τ_b about the mean values due to the complex influence of secondary flow cells on τ_b.

Yang and Lim (1998) presented an analytical method for the computation of boundary shear stress distributions acting on the flow perimeter of prismatic open channels. They introduced analytical equations which are valid for all channel aspect ratios and verified them using experimental shear stress data.

In this study, many point velocity measurements were taken throughout the entire cross-section within the fully developed boundary layer using a propeller-type velocity meter. The experiments were carried out separately for smooth and rough surfaces in open channel models. Using the universal logarithmic velocity distribution equation for both flow conditions, the shear stress was computed for the inner region, and the shear stress distribution along the cross section was investigated. The mean and maximum shear stresses and their positions along the cross section were determined for all flow conditions. Hence, the objective of this study was to obtain succinct expressions for shear stress distribution separately for smooth and rough surfaced prismatic open channels and covering a wide range of flow conditions.

DETERMINATION OF SHEAR STRESS

Because of the difficulties associated with direct measurement of the wall shear stress, τ_0, the shear velocity, u_*, is usually calculated by indirect methods. Preston (1954) developed a simple technique for measuring local shear on smooth boundaries in the turbulent boundary layer using a Pitot tube placed in contact with the surface. Wu and Rajaratnam (2000) presented a simple method for real time measurement of the bed shear stress for turbulent flow over uniformly rough boundaries with the help of a Pitot tube, based on the classical logarithmic velocity distribution equation. Ackerman and Hoover (2001) indicated that it is possible to measure the local shear stress quickly, consistently, and inexpensively by a Pitot-static tube. Another method used the water surface slope in order to compute the wall shear stress by $\tau_0 = \rho ghS$, where S is the water surface slope, h is the water depth and ρ is the water density (Kamphuis 1974).

K*ı*rkgöz (1989) computed shear velocities using the measured velocity distributions in the viscous sublayer. By assuming a linear velocity distribution in the viscous sublayer, the shear velocity can be derived from the Newton's law of viscosity as $u_* = \sqrt{\upsilon u/z}$ where u represents the point velocity in the viscous sublayer at a distance z from the bed and υ is the kinematics viscosity of the fluid. Starting out with an assumed velocity distribution, such as the law of the wall (as in Steffler *et al*. 1985), or a power law (as in Sarma *et al*. 1983), and implementing this distribution into the model: $\tau_0 = \mu du/dz - \rho u'v'$, where u' and v' are the turbulent velocity fluctuations (Nezu & Rodi 1986), we obtain commonly used method for determination of the shear stress, τ_0.

EXPERIMENTAL

Experiments were performed in a glass-walled laboratory channel which was 9.5 m long, 0.6 m wide and 0.6 m deep at the Hydraulics Laboratory of Erciyes University in Kayseri, Turkey (Fig. 1a). The existing channel bed was used directly for "smooth-wall" experiments. For "rough-surface" experiments, a plastic-doormat, with a height of 10 mm (k_s), was laid on top of the channel bottom (Fig. 1b). The flow rate of the water passing through the flume was measured with a UFM-400 type ultrasonic current meter mounted on the pipe transferring the water from a constant-head tank to the flume entrance. The channel bed slope was arranged by the slope screw and uniform flows were obtained using a downstream gate for controlling the water depth in the flume as shown in Figure 1.

Some details of the experiments for both "smooth" and "rough" surfaces are summarized in Table 1, in which Q is the flow rate (measured by the ultrasonic current meter), S is the water surface slope, h is the water depth, b/h is the flow aspect ratio, Fr is the Froude Number $\left(= V/\sqrt{gh}\right)$, V is the average cross-sectional velocity, and Re is the Reynold Number $(= 4VR/\upsilon)$, in which R is the hydraulic radius, defined as: R = a/P, where a is the cross-sectional area and P is the wetted perimeter.

Development of the boundary layer in a similar open channel flow was previously investigated by K*ı*rkgöz and Ard*ı*çl*ı*oğlu (1997) who suggested a new equation depending on the Froude number, the Reynolds number and the flow depth. Using this equation, the boundary layer development distances were calculated for all flow conditions. These distances changed from 2.0 to 5.2m for smooth surfaces and from 3.2 to 5.2m for rough surfaces. Therefore, the velocity and shear stress distributions were measured at 6.0 m downstream from the entrance, where the fully developed flow occurred for all types of flows studied.

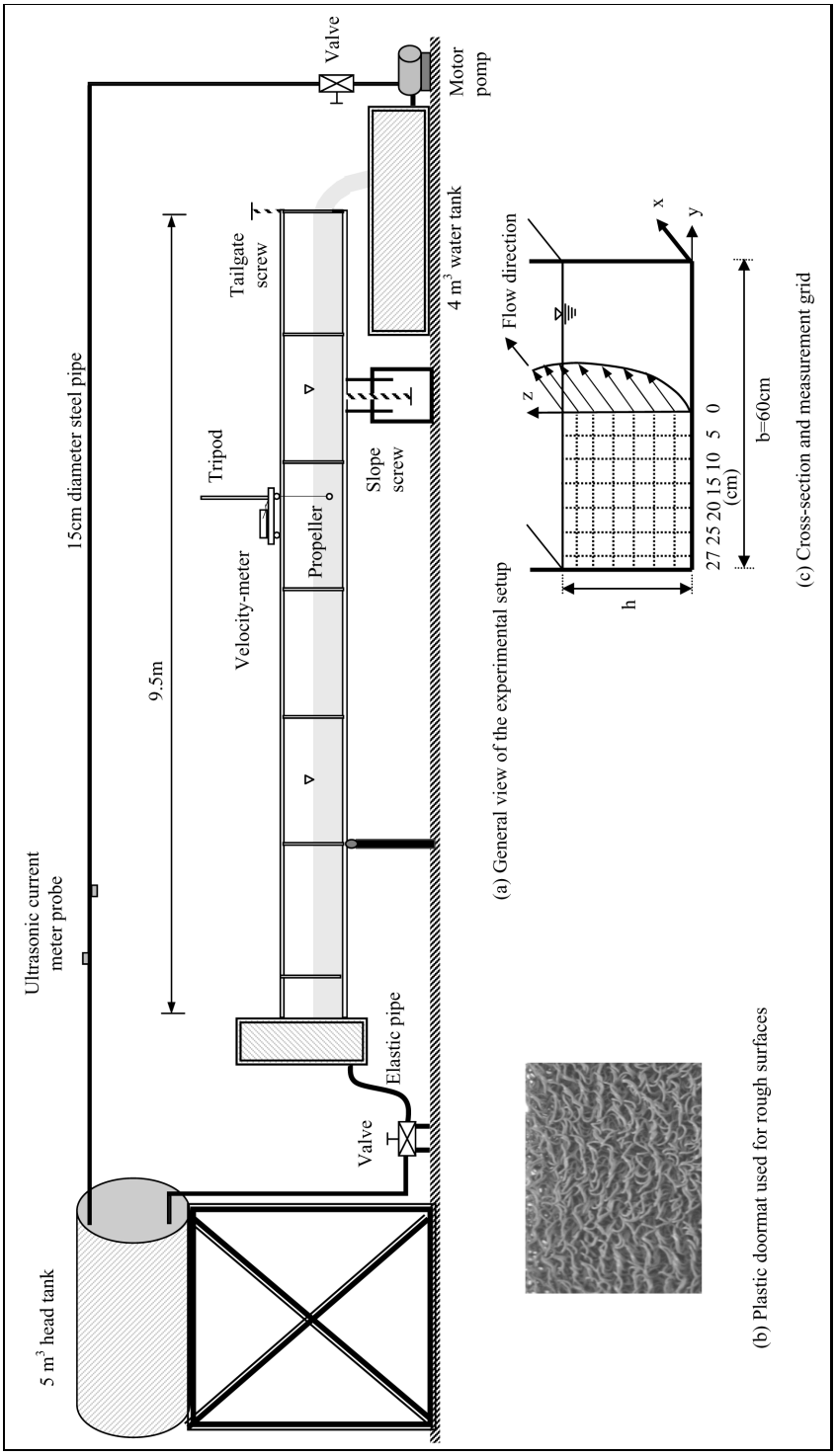

Figure 1: Laboratory flume

The velocities were measured by propeller-type velocity meter (Streamflo Velocity Meter 400) installed on a special frame able to move in any direction. Point velocity measurements were repeated three times with each taking a period of 10 seconds, and the mean value of these three readings was taken as the point velocity. The measuring head with a cage approximately 15mm diameter enabled readings to be taken in confined spaces. The system was highly sensitive, responding to velocities as low as 0.025 m/s with ±2% accuracy. Point velocity measurements were taken at various points on seven verticals (y = 0, 5, 10, 15, 20, 25, 27 cm, see Fig. 1c. Due to the symmetry, the velocity measurements were taken on only one side of the cross-section (Ardiçlioğlu 2006). For every vertical, measurements were taken from 7.5 mm over the flume bed with 10 mm increments up to the water surface. Free surface velocity was then estimated by regression of the upper two measurements.

Table 1: Description of the data used in the study

Smooth Surface							Rough Surface						
Test (1)	Disch. Q-(lt/s) (2)	Slope S (3)	Depth h-(cm) (3)	Aspect R. b/h (4)	Fr Num. (6)	Re Num. (7)	Test (1)	Disch. Q-(lt/s) (2)	Slope S (3)	Depth h-(cm) (3)	Aspect R. b/h (4)	Fr Num. (6)	Re Num. (7)
S1	8.18	0.0020	8.00	7.50	0.12	22825	R1	8.01	0.0020	9.40	6.38	0.14	33903
S2	8.24	0.0005	5.97	10.10	0.18	23411	R2	8.45	0.0005	6.04	9.93	0.24	33165
S3	10.23	0.0035	2.78	21.58	1.01	47135	R3	10.16	0.0035	5.00	12.00	0.48	50350
S4	10.95	0.0020	9.81	6.12	0.20	50318	R4	11.00	0.0020	9.04	6.64	0.22	51430
S5	11.92	0.0020	7.17	8.37	0.30	50762	R5	11.82	0.0020	11.81	5.08	0.17	54115
S6	12.39	0.0005	10.54	5.69	0.34	95485	R6	12.41	0.0005	8.79	6.83	0.22	49137
S7	12.47	0.0005	8.41	7.13	0.28	59233	R7	12.50	0.0005	10.17	5.90	0.23	61028
S8	13.65	0.0005	6.17	9.72	0.52	72902	R8	13.50	0.0005	6.48	9.26	0.41	61112
S9	15.42	0.0050	3.53	17.00	1.15	75136	R9	15.13	0.0050	5.28	11.40	0.59	66323
S10	17.00	0.0005	8.00	7.50	0.38	74017	R10	16.98	0.0050	8.04	7.46	0.43	84988
S11	18.98	0.0015	6.16	9.74	0.60	83204	R11	18.76	0.0015	7.33	8.19	0.48	84743
S12	19.25	0.0006	6.88	8.72	0.55	88759	R12	19.12	0.0006	7.78	7.71	0.45	84539
S13	20.16	0.0020	13.02	4.61	0.21	74237	R13	20.12	0.0020	13.11	4.58	0.24	85150
S14	21.29	0.0005	13.58	4.42	0.23	86245	R14	21.21	0.0005	14.14	4.24	0.22	87336
S15	21.83	0.0035	4.78	12.55	1.09	108212	R15	21.51	0.0035	7.13	8.42	0.55	93567
S16	26.07	0.0030	7.23	8.30	0.71	122447	R16	26.19	0.0030	8.33	7.20	0.56	115524
S17	34.00	0.0020	8.00	7.50	1.02	200554	R17	33.95	0.0020	9.56	6.28	0.59	144949
S18	34.04	0.0020	8.59	6.98	0.71	151600	R18	34.04	0.0005	8.32	7.21	0.69	141927
S19	34.19	0.0050	5.82	10.31	1.23	158374	R19	34.16	0.0044	8.11	7.40	0.74	146947
S20	34.33	0.0010	9.73	6.17	0.62	156996	R20	34.24	0.0010	9.96	6.02	0.56	144827
S21	38.00	0.0025	8.00	7.50	1.09	212964	R21	37.89	0.0047	8.41	7.13	0.77	160412
S22	39.42	0.0025	9.53	6.30	0.72	175610	R22	39.38	0.0025	9.98	6.01	0.64	166066
S23	40.84	0.0008	10.64	5.64	0.62	174449	R23	40.64	0.0008	11.14	5.39	0.53	158479
S24	42.02	0.0050	6.60	9.09	1.18	180897	R24	42.00	0.0050	9.18	6.54	0.68	158833

Disch.: Discharge, Aspect R.: Aspect Ratio, Num.: Number

RESULTS AND DISCUSSION

The shear stress occurring on the bottom of the channel was calculated using the logarithmic velocity distribution equation of von Karman-Prandtl, named "law of the wall"(von Karman 1930, Prandtl 1932), which is:

$$\frac{u}{u_*} = A \ln \frac{u_* z}{\upsilon} + B \tag{1}$$

where, A = $1/\chi$ (and, χ is the universal von Karman constant), B = a constant whose value depends on the physical nature of the wall surface, u is the local velocity at the point that is z units upwards from the solid bottom, u_* is the shear velocity, and υ is the kinematics viscosity of the fluid. The constants of the Eq. 1 were found to be: A = 2.5 and B = 5.5 from Nikuradse's (1932) experiments for hydraulically smooth pipe flow, and Keulegan (1938) assumed that the same values could be used for smooth open channel flow. In a recent study, Kırkgöz (1989) confirmed these results. Kırkgöz and Ardıçlıoğlu (1997) found that in the turbulent part of the inner region of developing and fully developed boundary layers on a smooth bed, the experimental velocity profiles agreed reasonably well with the logarithmic law of the wall distribution, with the magnitudes for these coefficients as: A = 2.44 and B = 5.5, which were almost the same as formerly suggested.

The velocity distribution on rough surfaces is affected by the grading, shape and spacing of the roughness elements of the surface. In dealing with the velocity distribution in rough-boundary flows, the most common practice has been to use Nikuradse's (1932) expression for fully rough turbulent flow in pipes, which is:

$$\frac{u}{u_*} = 2.5 \ln \frac{z}{k_s} + 8.5 \tag{2}$$

where, k_s = Nikuradse's original uniform sand grain roughness and z = the distance from the bottom of the roughness elements.

Using the logarithmic velocity distributions valid in the fully turbulent part of the inner region, which are given as Eqs. 1 and 2 for both smooth and rough surfaces, the bottom shear stresses were computed for all the seven vertical lines with all 48 different flow conditions. With the known values of A = 2.5 (χ = 0.4) and B = 5.5 for smooth surfaces, and using B = 8.5 for rough surfaces, u_* values, which best represented the overall data in the turbulent part of inner region, were determined. For the smooth surface, Test S13 is shown in Fig. 2a, and for the rough surface, Test R23 is given Fig. 2b. The dimensionless bottom shear stresses in addition to the cross-sectional mean and maximum shear stresses are summarized in Table 2.

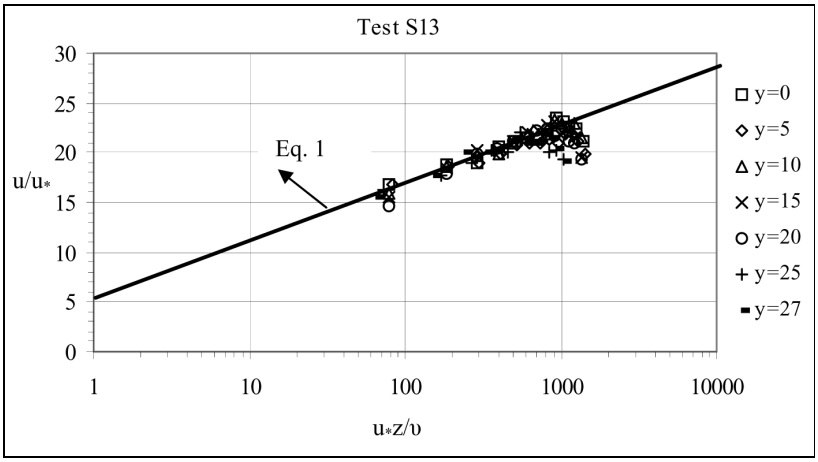

(a)

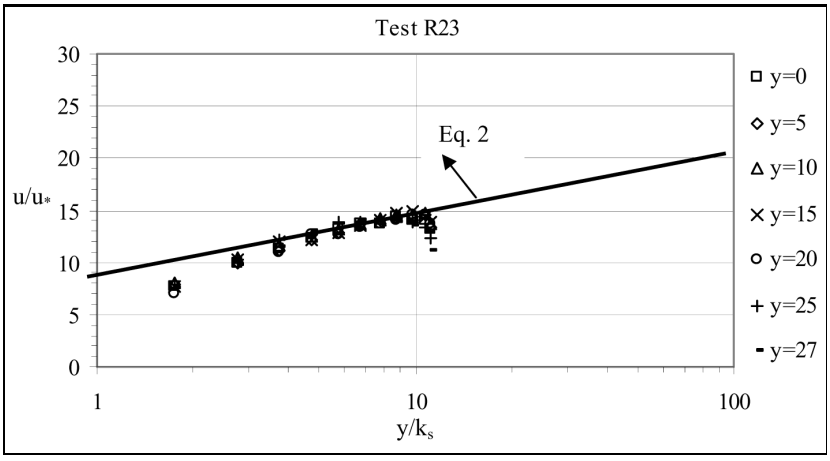

(b)

Figure 2: Law of the wall distribution for smooth (a) and rough (b) surfaces

It is a known fact that gravitational forces play a dominant role on the movement of open channel flow, as stated by Chow as follows: "The effect of gravity upon the state of flow is represented by a ratio of inertial forces to gravity forces. This ratio is given by the Froude number", and further: "It is believed that gravity action may have a definitive effect upon the flow resistance in channels at the turbulent flow range" (Chow 1959). Knight and Patel (1985) measured boundary shear stress distribution in fully developed turbulent flows in smooth rectangular ducts. Perturbations in these distributions were identified with multiple pairs of contra-rotating secondary flow cells. They reported that the number and distribution of these cells was correlated with the aspect ratio.

Guo and Julien (2002) theoretically investigated the bed and side wall shear stresses for rectangular open channels. Their analysis demonstrated that the boundary shear stress consisted of three components: gravity which caused the primary contribution, secondary currents and fluid shear stresses.

The relations between cross sectional mean shear stresses, aspect ratios (b/h) and Froude numbers (Fr) were established for smooth and rough surfaces using multiple regression analyses by the following expressions, respectively,

$$\tau_m = -0.043 - 0.053b/h + 2.06\,Fr \qquad \text{and} \tag{3}$$

$$\tau_m = -0.019 - 0.013b/h + 5.86\,Fr. \tag{4}$$

Table 2: Dimensionless shear stress τ_0/τ_m

Smooth Surface										Rough Surface									
Test	2y/b							τ_m	τ_{max}	Test	2y/b							τ_m	τ_{max}
	0	0.17	0.33	0.5	0.67	0.83	0.9	N/m²	N/m²		0	0.17	0.33	0.5	0.67	0.83	0.9	N/m²	N/m²
S1	1.18	1.18	1.07	1.00	0.91	0.88	0.78	0.036	0.042	R1	1.14	1.08	1.00	0.96	1.00	1.00	0.83	0.133	0.151
S2	1.08	1.08	1.03	1.00	1.00	0.93	0.88	0.064	0.069	R2	1.02	1.02	1.02	1.02	0.99	0.99	0.93	0.310	0.317
S3	1.07	1.07	1.01	1.03	1.02	0.98	0.82	0.899	0.961	R3	1.07	1.07	1.04	0.98	0.98	0.98	0.90	1.083	1.156
S4	1.12	1.12	1.04	1.02	1.00	0.93	0.77	0.106	0.119	R4	1.09	1.09	1.09	0.97	0.92	0.92	0.92	0.314	0.342
S5	1.12	1.12	1.04	1.04	1.04	0.86	0.77	0.188	0.210	R5	1.19	1.08	1.01	0.94	0.93	0.93	0.93	0.194	0.231
S6	1.03	1.08	1.06	1.01	0.99	0.99	0.84	0.112	0.121	R6	1.06	1.06	1.06	1.00	1.00	1.00	0.83	0.307	0.324
S7	1.07	1.07	1.07	0.99	0.99	0.99	0.84	0.158	0.169	R7	1.09	1.09	1.03	0.98	0.92	0.98	0.92	0.332	0.361
S8	1.08	1.08	1.06	0.99	0.97	0.95	0.87	0.449	0.484	R8	1.09	1.09	1.09	1.01	0.93	0.89	0.89	0.619	0.676
S9	1.04	1.06	1.07	1.07	1.02	0.96	0.76	1.344	1.444	R9	1.05	1.05	1.01	1.01	0.96	0.96	0.96	1.753	1.849
S10	1.15	1.15	1.03	1.01	0.95	0.89	0.82	0.281	0.324	R10	1.03	1.03	1.03	1.00	0.97	0.97	0.94	1.118	1.156
S11	1.07	1.11	1.05	0.97	0.90	0.98	0.92	0.564	0.625	R11	1.01	1.03	1.07	1.04	0.96	0.96	0.93	1.315	1.406
S12	1.05	1.09	1.06	1.04	0.94	0.94	0.88	0.537	0.586	R12	1.04	1.04	1.10	1.07	0.95	0.90	0.90	1.212	1.332
S13	1.06	1.14	1.05	1.05	1.03	0.88	0.80	0.136	0.156	R13	1.12	1.12	1.02	0.93	0.89	0.98	0.93	0.472	0.529
S14	1.07	1.10	1.04	1.02	0.93	0.99	0.85	0.181	0.199	R14	1.06	1.11	1.06	0.96	1.01	0.96	0.83	0.436	0.484
S15	1.09	1.11	1.04	1.03	0.97	0.93	0.83	1.448	1.608	R15	1.08	1.08	1.08	1.03	0.93	0.93	0.88	1.719	1.849
S16	1.07	1.15	1.09	1.06	0.95	0.87	0.81	0.828	0.949	R16	1.02	1.07	1.11	1.02	0.89	0.94	0.94	2.067	2.304
S17	1.08	1.06	1.03	1.02	0.98	0.95	0.87	1.796	1.936	R17	1.03	1.07	1.07	1.07	0.99	0.91	0.87	2.335	2.500
S18	1.02	1.06	1.04	1.01	1.04	0.93	0.90	0.945	1.005	R18	1.05	1.05	1.09	1.05	0.94	0.94	0.90	2.889	3.136
S19	1.12	1.09	1.08	1.07	0.97	0.87	0.80	2.025	2.275	R19	1.08	1.08	1.08	1.06	1.00	0.90	0.81	3.348	3.600
S20	1.05	1.12	1.05	1.03	0.98	0.92	0.85	0.860	0.961	R20	1.00	1.13	1.13	1.04	0.96	0.91	0.83	2.215	2.500
S21	1.09	1.08	1.02	0.99	0.99	0.93	0.90	1.952	2.134	R21	1.07	1.07	1.08	1.07	1.00	0.92	0.81	3.609	3.906
S22	1.10	1.10	1.03	0.97	0.97	0.91	0.91	1.053	1.156	R22	1.06	1.06	1.06	0.98	0.98	0.95	0.91	2.965	3.136
S23	1.05	1.12	1.05	0.98	0.92	0.96	0.93	0.884	0.992	R23	1.15	1.10	1.01	0.92	0.92	0.97	0.92	2.093	2.401
S24	1.06	1.10	1.06	1.03	0.90	0.95	0.89	2.148	2.362	R24	1.06	1.06	1.06	1.02	0.99	0.92	0.89	3.172	3.364

The determination coefficients of these best fit regression equations (Eqs. 3 and 4) are: $R^2 = 0.96$ and 0.97, respectively. Efforts were made to determine the most meaningful expressions where the average shear stress was the dependent variable. For this purpose, expressions containing single and multiple independent variables have been tried. The independent variables were; the Reynolds number, Re, the aspect ratio, b/h and the Froude number, Fr. The results of the multiple linear regressions using aspect ratio and Froude number as independent variables to predict mean shear stresses τ_m yielded high correlations for both smooth and rough surfaces. In Figure 3, the relationships between observed and calculated cross-sectional mean shear stresses as predicted by Eq. 3 and 4 are given. As shown in the figure, the observed and predicted values show good agreement.

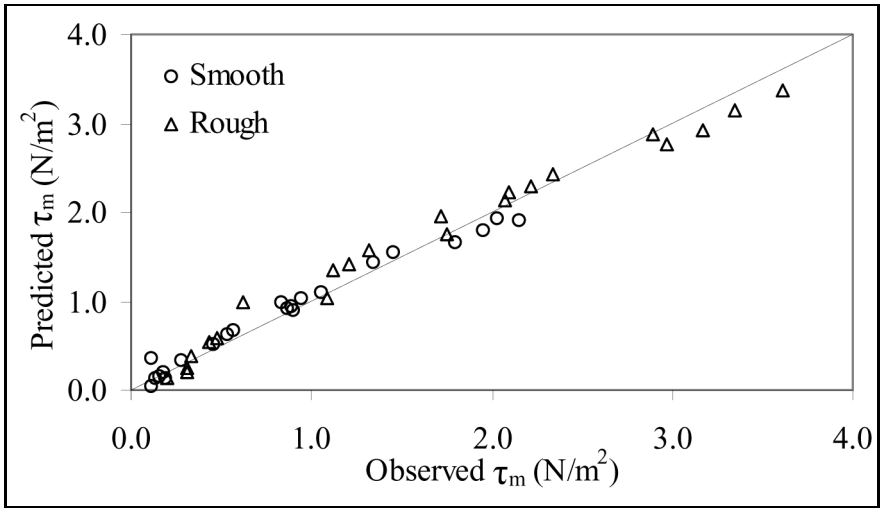

Figure 3: Relation between observed and predicted cross-sectional mean shear stresses, τ_m

For all the flow conditions formed in the setup, the shear stress distribution along the cross section was investigated. Figure 4 shows these variations along the cross section for fully developed flow conditions. In this figure, the dimensionless shear stress distribution shows an oscillatory behavior which could be explained by the positioning of the secondary current cells created by the corner boundaries in straight channels. This distribution can be determined as a second degree polynomial as shown in Figure 4. The regression equation fitted to this relation is:

$$\frac{\tau_0}{\tau_m} = -0.247\,(2y/b)^2 + 0.007\,(2y/b) + 1.079 \qquad (5)$$

whose determination coefficient is: $R^2 = 0.75$. The maximum shear stress on the bed was found to be about 6 - 15% greater than the mean bed shear stress for

smooth surfaces and 5 - 15% grater than the mean bed shear stress for rough surfaces. Knight and Patel (1985) reported that the maximum bottom shear stress was 13% greater than the average value. In all of the flow conditions, the maximum shear stress occurred mostly at the middle section of the channel and decreased close to the side wall.

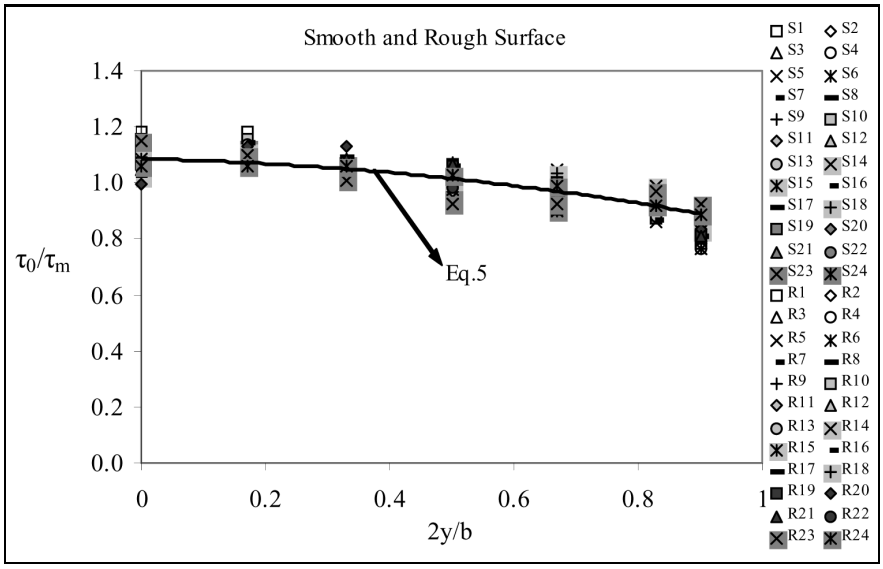

Figure 4: Variations of τ_0 / τ_m along the cross section

CONCLUSIONS

Boundary shear stress distributions have been experimentally determined in fully developed turbulent flows separately for smooth-surfaced and rough-surfaced rectangular open channels. Using the logarithmic velocity distributions valid in the fully turbulent part of the inner region, the bottom shear stresses were calculated over seven vertical lines in half of the cross-section for 48 different flow conditions. The relationships between cross sectional mean shear stresses, aspect ratio (b/h) and Froude number (Fr) were established using multiple regression analyses for smooth and rough surfaces. As a result of the multiple linear regressions, high correlations were obtained for both surfaces. The dimensionless shear stress distributions, τ_0/τ_m, along the cross-section are meaningfully represented by second degree polynomials for both surface conditions. The maximum shear stress on the bed was found to be about 6 to 20% greater than the mean bed shear stress for smooth surfaces and 2 to 16% grater for rough surfaces. For all of the flow conditions, the maximum shear stress occurred mostly in the middle section of the channel.

I. Appendix

a = cross sectional area,

A = $1/\chi$ (inverse von-Karman constant),

b = channel width

B = velocity distribution constant,

b/h = aspect ratio,

Fr = Froude number,

g = gravitational acceleration,

h = flow depth,

Q = flow discharge,

R = hydraulic radius,

R^2 = determination coefficient,

Re = Reynolds number,

S = water surface slope,

u = local velocity,

u_* = shear velocity,

V = average flow velocity,

x = distance from the channel entrance,

y = transverse horizontal distance from the centerline of channel bed,

z = vertical distance from channel bed,

μ = dynamic viscosity,

ρ = water density,

$\tau_0, \tau_m, \tau_{max}$ = local bed, averaged bed and maximum shear stress,

υ = kinematics viscosity, and

χ = von-Karman constant.

REFERENCES

Abaza, K.A. & Al-Khatib, I.A. 2003. Generalization of shear stress distribution in rectangular compound channels. Turkish Journal of Engineering and Environmental Science **27:** 409-421.

Ackerman, J.D. & Hoover, T.M. 2001. Measurements of local bed shear stress in stream using a Preston-static tube. Limnology Oceanography **46(8):** 2080-2087.

Al-Khatib, I.A. & Dmadi, N.M. 1999. Boundary shear stress in rectangular compound channels. Turkish Journal of Engineering and Environmental Science **23:** 9-18.

Ardıçlıoğlu, M. 2006. Velocity -- discharge measurements in open channel flow. Technical Journal, Turkish Chamber of Civil Engineers **17(1):** 3805-3808.

Biron, P., Lane, S.N., Roy, A.G., Bradbrook, K.F.& Richards, K.S. 1997. Sensitivity of bed shear stress estimated from vertical velocity profiles: problem of sampling resolution. Earth Surface Processes and Landforms **23:** 133-139.

Chow, V. T. 1959. Open Channel Hydraulics. McGraw-Hill Book Co., New York, NY, USA.

Guo, J. & Julien, P.Y. 2002. Boundary shear stress in smooth rectangular open-channels. Advances in Hydraulics and Water Engineering. Proceedings of the 13th IAHR-APD Congress, Singapore.

Karman, T. von 1930. Mechanische Ahnlichkeit und Turbulenz, G\"{o}ttinger Nachrichten, Mathematic-Physikalische Klasse: 58-60.

Kamphuis, J. W. 1974. Determination of sand roughness for fixed beds. Journal of Hydraulic Research **12(2):** 193-203.

Keulegan, G.H. 1938. Laws of turbulent flow in open channels. Journal of Research, Nat. Bureau of Standards, Washington D.C. **21:** 707-741.

Kırkgöz, M.S. 1989. Tubulent velocity profiles for smooth and rough open channel flow. Journal of Hydraulic Engineering, ASCE **115(11):** 1543-1561.

Kırkgöz, M.S. & Ardıçlıoğlu, M. 1997. Velocity profiles of developing and developed open channel flow. Journal of Hydraulic Engineering, ASCE **123(12):** 1099-1105.

Knight, D.W. & Patel, H.S. 1985. Boundary shear in smooth rectangular ducts. Journal of Hydraulic Engineering, ASCE **111(1):** 29-47.

Knight, D.W., Yuen, K.W.H. & Achamid, A.A.F. 1994. Boundary shear stress distributions in open channel flow. In: Bevon, K., Chakin P. & Willbank J.(Eds.). Physical Mechanisms of Mixing and Transport in the Environment. pp. 51-87. J. Wiley, New York, USA.

Nezu, I. & Rodi, W. 1986. Open channel measurements with a Laser Doppler Anemometer. Journal of Hydraulic Engineering, ASCE **112(4):** 335-355.

Nezu, I., Tominaga, A. & Nakagawa, H. 1993. Field measurements of secondary currents in straight rivers. Journal of Hydraulic Engineering, ASCE **119(4):** 598-614.

Nikuradse, J. 1932. Gesetzmassigkeiten der turbulent Str\"{o}mung in glatten Rohren, Forsch. Geb. Ing.-Wes., Heft 356.

Prandtl L. 1932. Zur turbulenten Str\"{o}mung in Rohren und langs platten, Ergebnisse der Aerodynamischen Versuchsanstalt zu G\"{o}ttingen, **4**, 18-29.

Preston, J.H. 1954. The determination of turbulent skin friction by means of pitot tubes. Journal of the Royal Aeronautical Society **58:** 109-121.

Rhodes, D.G. & Knight, D.W. 1994. Distribution of shear force on boundary of smooth rectangular duct Journal of Hydraulic Engineering, ASCE **120(7):** 787-7807.

Sarma, K.V.N., Lakshminarayana, P. & Rao, N.S.L. 1983. Velocity distribution in smooth rectangular open channels. Journal of Hydraulic Engineering, ASCE **109(2):** 270-289.

Steffler, P.M., Rjaratnam, N. & Peterson, A.W. 1985. LDA measurements in open channel. J. Journal of Hydraulic Engineering, ASCE **111(1):** 119-130.

Wu, A. & Rajaratnam N. 2000. A simple method for measuring shear stress on rough boundaries. Journal of Hydraulic Research **38:** 399-400.

Yang, S.Q. & Lim, S.Y. 1998. Boundary shear stress distributions in smooth rectangular open channel flows. Proc. Proceedings of the Institution of Civil Engineers- Water, Maritime & Energy **130:** 163-173.

Zheng, Y. & Jin, Y.C. 1998. Boundary shear in rectangular ducts and channels. Journal of Hydraulic Engineering, ASCE **124(1):** 86-89.

Submitted : *8/6/2004*
Revised : *30/8/2005*
Accepted : *11/10/2005*

توزيع إجهاد القص المقطعي لتدفق السوائل على امتداد القنوات المفتوحة ذات الأسطح الملساء والأسطح الخشنة

مهمت اردیکلیوکلو[1]، کالب سیکین[2] وریسیب یورتال[2]

[1]قسم الهندسة المدنية، جامعة أركيز، تركيا
[2]قسم الهندسة البيئية والمدنية، جامعة كوكوروفا، تركيا

خلاصة

تم قياس توزيع إجهاد القص لمقاطع مختلفة في منطقة طبقة التدفق المتكامل على طول قنوات مفتوحة مستطيلة المقطع وذات أسطح ملساء وقنوات ذات أسطح خشنة، أخذت قياسات السرعة لنوعين من الأسطح ولـ 48 حالة مختلفة من حيث ظروف التدفق وأبعاد مقطع القناة، تم حساب إجهاد القص الموضعي بطريقة التوزيع اللوغارتمي العام. أظهرت النتائج أن توزيع إجهاد القص لكل مقطع على امتداد القناة يتبع بدقة العلاقة متعددة الحدود من الدرجة الثانية وأن قيمة الإجهاد الأقصى في القنوات الملساء أكبر من قيمة معدل الإجهاد لكل مقطع بمقدار 6–20٪ وبمقدار 2–12٪ للقنوات ذات الأسطح الخشنة.